New Journal of Physics
The open-access journal for physics

Using TIRF microscopy to quantify and confirm efficient mass transfer at the substrate surface of the chemistrode

Delai Chen, Wenbin Du and Rustem F Ismagilov[1]
Department of Chemistry and Institute for Biophysical Dynamics, The University of Chicago, 929 East 57th Street, Chicago, IL 60637, USA
E-mail: r-ismagilov@uchicago.edu

New Journal of Physics **11** (2009) 075017 (9pp)
Received 20 January 2009
Published 31 July 2009
Online at http://www.njp.org/
doi:10.1088/1367-2630/11/7/075017

Abstract. This paper describes experiments for characterizing mass transfer at the hydrophilic surface of the substrate in a chemistrode. The chemistrode uses microfluidic plugs to deliver pulses of chemicals to a substrate with high temporal resolution, which requires efficient mass transfer between the wetting layer and the hydrophilic surface of the substrate. Here, total internal reflection fluorescence microscopy (TIRFM) was used to image the hydrophilic surface of the substrate as plugs were made to flow over it. The surface of the substrate was rapidly saturated with a fluorescent dye as the fluroesecent plugs passed over the substrate, confirming effective mass transfer between the wetting layer and the surface of the substrate. The dynamics of saturation are consistent from cycle to cycle, indicating that the chemistrode can stimulate surfaces with high reproducibility. The number of plugs required to reach 90% saturation of the hydrophilic surface of the substrate, $\phi(90\%)$, only weakly depended on experimental conditions (the Péclet number or the capillary number). Furthermore, over a wide range of operating conditions, $\phi(90\%)$ was less than 4. These results are useful for improving the chemistrode and for understanding other phenomena that involve diffusional transfer in multiphase or recirculating flows near surfaces.

[1] Author to whom any correspondence should be addressed.

Contents

1. Introduction 2
2. Materials and methods 2
3. Results and discussion 4
4. Conclusions 8
Acknowledgments 8
References 8

1. Introduction

This paper presents experiments to visualize mass transfer of dye molecules from the incoming solution in the wetting layer to the hydrophilic surface of the substrate in a chemistrode [1]. Two-phase microfluidics has been used to transport solutions as discrete units without loss of temporal resolution in applications ranging from chemical synthesis to sampling from biological tissues [1–9]. The chemistrode is a recently developed plug-based microfluidic device enabling stimulation and recording with high spatial and temporal resolution [1]. Pulses of chemicals are encapsulated in plugs, droplets that are nanoliters in volume surrounded by a fluorocarbon carrier fluid, and delivered to a substrate with a hydrophilic surface. The response plugs formed on the surface capture chemical signals secreted by the substrate in response to the pulses. The chemistrode relies on controlled coalescence of plugs with the wetting layer on a stationary surface and reformation of response plugs [10], a process different from the well-documented coalescence between droplets in an open volume [11] or between a plug and a flowing stream [12]. For the chemistrode to stimulate and record from the substrate, chemicals must be exchanged between the wetting layer and the hydrophilic surface of the substrate (figure 1).

The previous report [1] used confocal microscopy to image the wetting layer, specifically to observe the exchange of dye molecules between the incoming solution and the wetting layer. Here, we use total internal reflection fluorescence microscopy (TIRFM) to image the hydrophilic surface itself (figure 1). TIRFM provides optical sectioning of $<100\,\mathrm{nm}$ thickness [13] above the glass–solution interface and completely eliminated interference from the bulk solutions in the wetting layer and the incoming plugs.

2. Materials and methods

We fabricated the chemistrode according to previously reported methods [1]. A V-shaped channel, with a cross section of $300\,\mu\mathrm{m} \times 300\,\mu\mathrm{m}$, was fabricated by rapid prototyping in poly(dimethylsiloxane) (PDMS) [14]. Microchannels were rendered hydrophobic and fluorophilic by flowing N_2-containing tridecafluoro-1,1,2,2-tetrahydrooctyl-1-trichlorosilane (United Chemical Technologies, Bristol, PA) vapor for 1 h into a device freshly sealed by plasma oxidation. Next, the device was carefully cut using a blade at the cross point of the 'V' channel to expose an opening. Teflon tubing (Stranco Products, Bolingbrook, IL), with an inner diameter (I.D.) of $237.5\,\mu\mathrm{m}$ and outer diameter (O.D.) of $287.5\,\mu\mathrm{m}$, was inserted into the channels to facilitate the transport of plugs (figure 1(a)). The gap between the Teflon tubing and the surrounding PDMS was filled with half-cured PDMS glue (Dow–Corning Sylgard 184 A

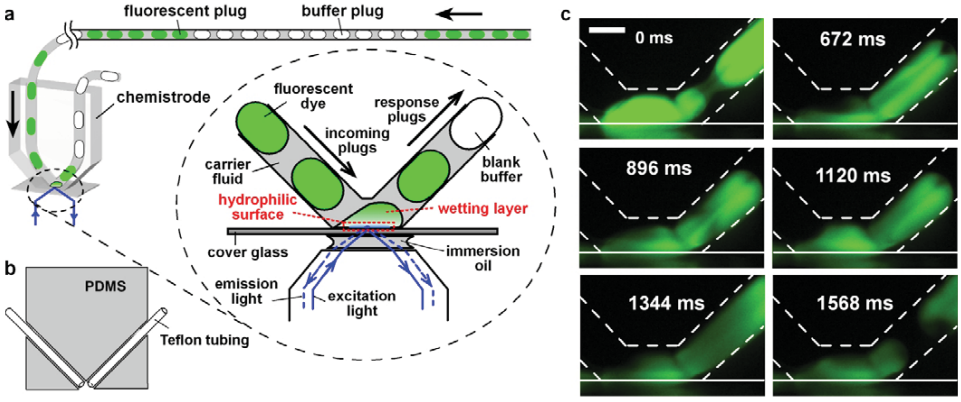

Figure 1. The experimental set-up for measuring the diffusion of dye molecules from the incoming solution in the wetting layer to the hydrophilic surface on the cover glass. (a) A successive series of 5 fluorescent plugs alternating with 10 blank buffer plugs was passed into the chemistrode and allowed to pass over the hydrophilic surface of the glass slide. The concentration of the fluorescent dye on the hydrophilic surface was monitored by TIRFM (zoomed-in region). (b) A schematic diagram of the microfabricated chemistrode device. (c) Fluorescence microscopic images show recirculation occurring in the wetting layer as buffer plugs passed over the surface of the hydrophilic substrate. At 0 ms, the center of the wetting layer was fluorescent, but at 672 ms, the center of the wetting layer was mostly non-fluorescent. Recirculation was evident from the eddies present at 672 and 896 ms and is also shown in movies S1 and S2, available from stacks.iop.org/NJP/11/075017/mmedia. The center of the wetting layer became fluorescent again at 1120 ms. The flow velocity was: 1.0 mm s^{-1}. The scale bar represents 200 μm.

and B at a ratio of 10:1, cured at 110 °C for 110 s), and then the device was baked at 65 °C to fully cure the PDMS glue.

The array of 5 fluorescent plugs alternating with 10 buffer plugs (figure 1(b)) was fabricated by using a computer-controlled syringe pump to alternately aspirate the carrier fluid and the corresponding aqueous solution into a piece of Teflon tubing (with an I.D. of 237.5 μm and an O.D. of 287.5 μm). The volume of each aqueous plug and the volume of the carrier fluid between two adjacent plugs were both 30 nl. The fluorescent solution was 1 μM Alexa Fluor ®g488 5-TFP (Invitrogen, Eugene, OR) dissolved in 1 × PBS (pH 7.4), hereafter referred to as Alexa Fluor®-488. The solution in buffer plugs was 1 × PBS (pH 7.4). For experiments involving changing the viscosity of aqueous solutions, glycerol (Fisher Scientific, Fair Lawn, NJ) was added to the aqueous solutions to achieve final mass percentages of 20, 30, 40, 50 and 60% in the respective solutions. We used the viscosity of the corresponding glycerol concentration in water [15] for the calculation of the capillary number, *Ca*. The carrier fluid in all experiments was 0.1 mg ml^{-1} triethyleneglycol mono [1H,1H-perfluorooctyl] ether [16] in FC3283 (3M Belgium). The interfacial tension between the carrier fluid and water was measured to be 21.2 mN m^{-1}, and this value was used for calculating *Ca*. For calculation of the Péclet numbers, the diffusion constant of Alexa Fluor®-488 in PBS buffer was approximated to 2×10^{-10} m^2 s^{-1}, as has been reported previously [17].

TIRFM experiments were performed on an Olympus IX81 TIRFM-SP microscope, using a Plan APO 60× oil objective, NA 1.45. The dye was excited by an argon 488 nm laser source. Images were acquired and analyzed using MetaMorph version 6.2r6. A culture dish with a glass bottom (No. 1; MatTek Corporation, Ashland, MA) was placed on the sample stage of the microscope. The glass bottom of the dish was made hydrophilic by plasma oxidation using a Plasma Prep II plasma cleaner before the experiment. A chemistrode was placed on top of the cover glass and held in place with a micromanipulator during the experiment. Flow of aqueous solution or plugs into the chemistrode was initiated by using a PHD 2000 syringe pump (Harvard Apparatus, Holliston, MA).

To visualize recirculation in the wetting layer, fluorescent plugs and buffer plugs were continuously generated in a microfluidic device and transported to the chemistrode as previously described [1]. The fluorescent plugs contained 200 μM fluorescein in 1× PBS buffer (pH 7.4); the buffer plugs consisted of 1× PBS solution (pH 7.4). Fluorescent images were taken with a GFP filter on a Leica DMI RE2 microscope equipped with a cooled CCD camera ORCA ERG 1394 (Hamamatsu Photonics, Hamamatsu City, Japan) and a 10× objective. An exposure time of 5 ms was used. The same scaling of intensities was applied to the whole area of all images in figure 1(c) and movie S1 (available from stacks.iop.org/NJP/11/075017/mmedia) to enhance contrast. For movie S2, plugs of the buffer were generated in a T-junction PDMS device and delivered to the chemistrode via a piece of 200 μm I.D. Teflon tubing. The volumetric flow rate for both the buffer and carrier streams was 20 μl min^{-1}, and the total flow rate was 40 μl min^{-1}. Pulses of fluorescein solution with well-defined injection time (40 ms) and intervals were generated and delivered to the substrate surface by using a microinjector. A LabVIEW program was used to control the microinjector for automatic operation. Images were taken by using a high-speed Phantom 7.1 camera (Vision Research) at 1000 fps (movie S2). Details of the experiment for movie S2 have been previously described in [1].

3. Results and discussion

We first determined whether complete saturation of the hydrophilic surface can be reached in the chemistrode. We used TIRFM to monitor the diffusion of Alexa Fluor®-488 from the incoming solution of the wetting layer to the hydrophilic surface. To establish the fluorescence intensity of a hydrophilic surface completely saturated with the Alexa Fluor®-488 solution, we passed the Alexa Fluor®-488 solution into the chemistrode without carrier fluid present. The solution was allowed to flow at 2 μl min^{-1} for over 1 min and then the TIRFM measurement was taken to make sure the intensity had stabilized and reached saturation.

We then determined whether complete saturation of the hydrophilic surface can be reached over a range of different flow velocities and viscosities. We monitored the TIRFM intensity while the repetitive arrays of 5 fluorescent plugs, alternating with 10 buffer plugs, were passed over the hydrophilic surface at volumetric flow rates ranging from 1.0 to 40 μl min^{-1} (corresponding to flow velocities from 0.50 to 21 mm s^{-1}) and with viscosities of the plugs of 0.882 and 3.12 mPa s, respectively. The TIRFM intensities reached under these conditions were essentially the same as the intensity of the completely saturated surface (with coefficients of variation of 2.4 and 3.5% for solutions in PBS and 40% glycerol/PBS, respectively), indicating that 100% saturation was reached under all the tested conditions (figure 2(b)).

Next, we evaluated the number of plugs required to reach complete (90%) saturation of the hydrophilic surface of the substrate, $\phi(90\%)$, and found $\phi(90\%) < 4$ under all these conditions. We calculated $\phi(90\%)$ by normalizing the time required for the TIRFM intensity to reach

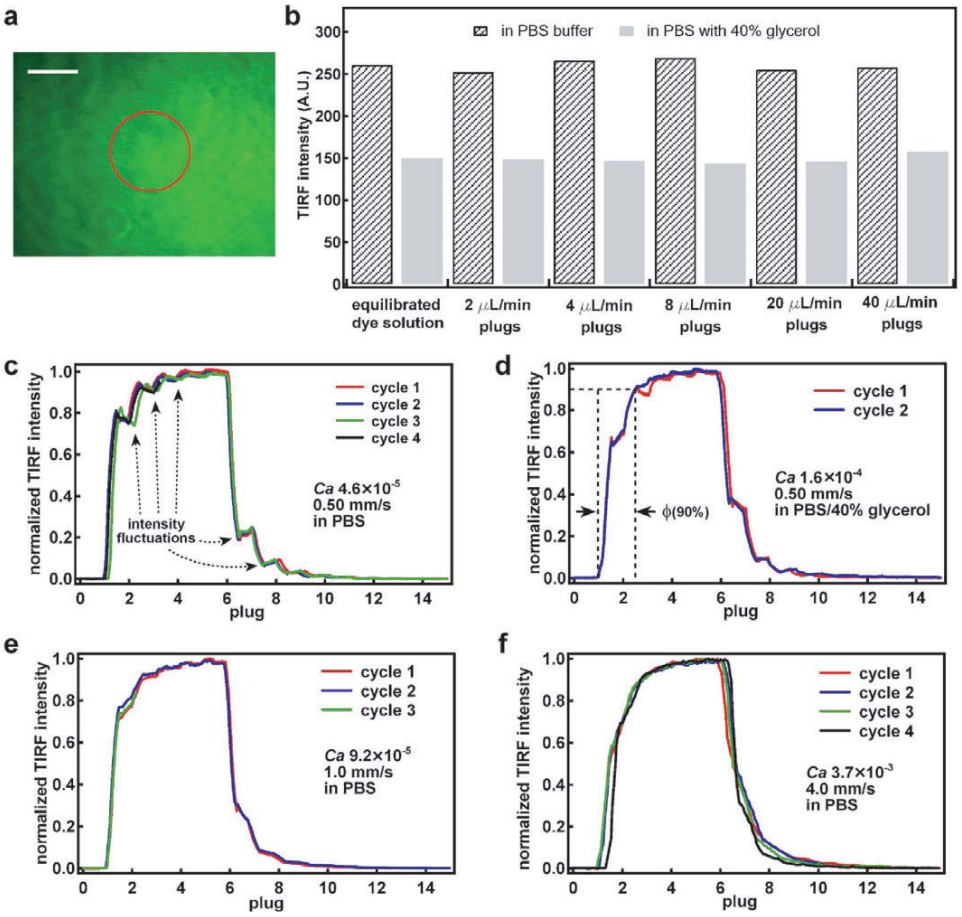

Figure 2. Complete saturation (90%) of the fluorescent dye on the hydrophilic surface was reached in less than 4 plugs over all measured conditions with high reproducibility ($<3.5\%$ coefficient of variation among cycles). (a) A typical TIRFM image of the hydrophilic surface in the chemistrode. The scale bar is 75 μm. The red circle indicates the region of interest in which the fluorescence intensity was averaged for analysis of surface saturation. (b) TIRFM intensity of plugs equaled that of the dye solution equilibrated on the hydrophilic surface at all measured flow velocities and viscosities. (c–f) Traces of TIRF intensity of plugs passed at different velocities and viscosities. The number of plugs required to reach complete (90%) saturation of the hydrophilic surface, $\phi(90\%)$, was always <4. Fluctuations in TIRFM intensity at low flow rates and low viscosity (c–e) indicated recirculation between the corners of the wetting layer and the center. Interfacial tension $= 21.2\,\mathrm{mN\,m^{-1}}$; viscosity $= 0.882\,\mathrm{mPa\,s}$ in (c, e, f); and viscosity $= 3.12\,\mathrm{mPa\,s}$ in (d). Overlapping lines for traces of repeat cycles indicated high reproducibility for stimulation of the hydrophilic substrate with the chemistrode.

90% saturation with the time required for one plug, and the carrier fluid between it and the next plug, to pass over the hydrophilic surface (figure 2(d)). Because the trace of TIRFM intensity was continuous, non-integral $\phi(90\%)$ values were often obtained. In all these cases, complete saturation of the surface was obtained within 1–4 plugs.

We noted that the traces of fluorescence intensities were highly reproducible among different cycles of plugs passing over the hydrophilic surface. The TIRFM intensity on the hydrophilic surface increased rapidly as the first fluorescent plug passed over the surface, and the intensity continued to increase gradually and reached saturation as subsequent fluorescent plugs passed over the surface (figures 2(c)–(f)). After the first buffer plug passed over the surface, the TIRFM intensity dropped quickly and then gradually reached the baseline. The dynamics of saturation of the hydrophilic surface with fluorescent dye was very similar to the dynamics of saturation by buffer plugs, as shown by the similarities in intensity fluctuations for plugs 1–4 with those of plugs 6–10 (figures 2(c)–(f)). Furthermore, the dynamics of saturation were very similar among repeated cycles (figures 2(c)–(f)), indicating that the chemistrode can be used to stimulate the surface of the hydrophilic substrate with very high reproducibility.

We observed an interesting effect of the capillary number on the dynamics of saturation of the hydrophilic surface. The dimensionless capillary number, Ca, is defined as $Ca = U\eta/\sigma$, where U ($\mathrm{m\,s^{-1}}$) is the flow velocity, η ($\mathrm{kg\,m^{-1}\,s^{-1}}$) is the dynamic viscosity and σ ($\mathrm{N\,m^{-1}}$) is the interfacial tension between the carrier fluid and the aqueous solution in a plug. At low values of Ca, there were significant fluctuations in the traces of TIRFM intensities during the passage of the fluorescent and buffer plugs over the surface of the substrate (figure 2(c), $Ca = 2.1 \times 10^{-5}$). We hypothesize that these fluctuations were due to recirculation (movie S2, available from stacks.iop.org/NJP/11/075017/mmedia) within the wetting layer that transported solution from the edges of the wetting layer to the center. In experiments imaging the chemistrode from the side (figure 1(c)), we have observed recirculation that redistributed fluorescent material in the wetting layer during the time between formation of response plugs (movie S1). Upon the passage of the first buffer plug, the center of the wetting layer was non-fluorescent, and the majority of fluorescence was close to the bottom of the wetting layer and on the side closer to the site of formation of response plugs. The eddies of fluorescence patterns also indicated recirculation, which brought the fluorescent dye to the center of the wetting layer (figure 1(c)). The fluctuations, which slowed down the exchange of dyes, were absent at higher values of Ca (figure 2(f)). The recirculation in the wetting layer was recorded more clearly in movie S2, in which a pulse of the fluorescence released from the substrate was sampled by the response plugs [1].

We found that $\phi(90\%)$ only weakly depended on the experimental parameters. To identify the parameters affecting the dynamics of saturation of the hydrophilic surface, we performed additional experiments with viscosities of the aqueous solution ranging from 0.88 to 9.0 mPa s and average flow velocities ranging up to $42\,\mathrm{mm\,s^{-1}}$, and determined $\phi(90\%)$ for each experiment. Ca in these experiments changed by over ~400-fold, from $\sim 2 \times 10^{-5}$ to $\sim 7 \times 10^{3}$, whereas $\phi(90\%)$ remained between 1 and 4 (figure 3). There appeared to be a log–linear relationship between Ca and $\phi(90\%)$: the data roughly fit a curve described by the function $\phi(90\%) = a\ln(Ca) + b$. We do not expect a correlation to the Reynolds number in these experiments, because the mass transfer occurred near the solid–liquid interface under low Reynolds number (between 0.1 and 10). We confirmed this prediction by plotting $\phi(90\%)$ versus Re or $\ln(Re)$, and we calculated R^2 based on the linear regression fit to the data points. In both cases, $R^2 < 0.55$, indicating a poor correlation between $\phi(90\%)$ and Re.

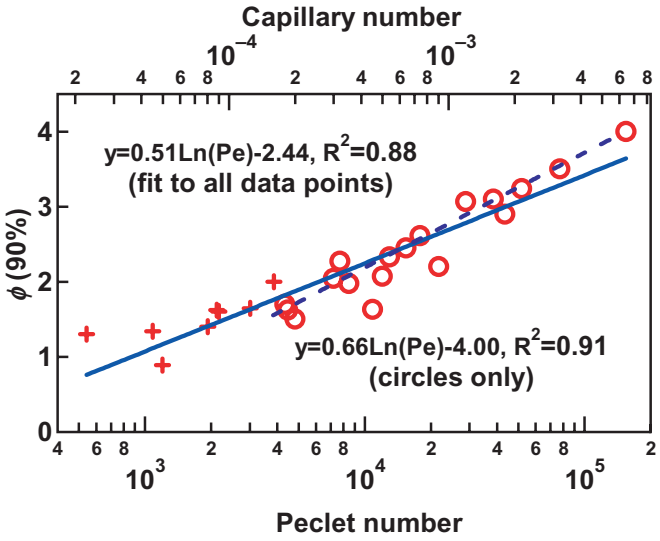

Figure 3. The number of plugs required to reach 90% saturation, $\phi(90\%)$, ranges from 1 to 4 over ~400-fold change in the capillary number or the Péclet number. When $\phi(90\%)$ was plotted against Pe on the lower horizontal axis and Ca on the upper horizontal axis, data points with $Ca > 2 \times 10^{-4}$ (circles, dashed line) were a slightly better fit to the log-linear relationship than the data set that also included points with $Ca < 2 \times 10^{-4}$ (crosses, solid line).

These experiments, however, did not differentiate between Ca and the Péclet number. The Péclet number is defined as $Pe = wU/D$, where Pe is the dimensionless Péclet number, w (m) is the characteristic length of the channel and D ($m^2\ s^{-1}$) is the diffusion coefficient of Alexa Fluor®-488. With the approximation that the Einstein–Sutherland equation can be applied to Alexa Fluor®-488 [18], D is proportional to $1/\eta$ for a spherical molecule. Because σ and w were kept constant in these experiments, $Ca = \eta U/\sigma \propto U/D \propto wU/D$; thus, Pe was proportional to Ca in these experiments.

The origin of this observed dependence between Pe and $\phi(90\%)$ is unknown. The relationship between Pe and $\phi(90\%)$ in this experiment was similar to the relationship between Pe and the time required to achieve 90% mixing by chaotic advection in plugs, $t_{90\%}$. In chaotic advection, $t_{90\%}$ is proportional to $(1/U)\ln(Pe)$ [19–22]; the number of plugs passing the channel during the mixing time, $\phi_{90\%(\text{mixing})}$, is proportional to $\ln(Pe)$: $\phi_{90\%(\text{mixing})} = t_{90\%}/(l/U) = l\ln(Pe)$ [21], where l (m) is the center-to-center distance between two adjacent plugs. In chaotic advection, the decrease in striation thickness by Baker's transformation [23, 24] gives rise to the dependence between $t_{90\%}$ and Pe [19]. It is possible that a similar mechanism exists to reduce the diffusion thickness of the wetting layer at the hydrophilic surface by a constant factor with every plug. Previous studies on coalescence between an incoming plug and the wetting layer in the chemistrode have observed a critical capillary number, $Ca_{\text{crit}} \sim 2\text{–}3 \times 10^{-4}$, which separates two regimes in which the rupture of the thin film of carrier fluid starts (i) from the nose region (i.e. the point of contact between the incoming plug and the wetting layer) or (ii) from the hydrophilic surface, respectively [10]. Interestingly, the fit of $\phi(90\%)$ to Ca was slightly improved when we used only the data

with values of Ca above 2×10^{-4}, but the significance of this observation remains to be investigated.

4. Conclusions

We confirmed that the incoming solution of the fluorescent dye in the wetting layer of the chemistrode rapidly saturated the hydrophilic surface and this phenomenon was reproducible from cycle to cycle. The number of plugs required to reach complete surface saturation, $\phi(90\%)$, was always less than 4 over a wide range of operating conditions. $\phi(90\%)$ determines the temporal resolution that can be achieved with the chemistrode and is important for applications involving stimulation and recording with high temporal resolution. Furthermore, $\phi(90\%)$ only weakly depended on experimental conditions (Pe or Ca). This dependence is very convenient for the use of the chemistrode, because operating parameters can be changed without a large impact on mass transfer at the surface. The origins of this dependence remain to be explored theoretically. Although mass transfer at a surface in a simple shear flow is understood well [25–28], mass transfer in this system is made more complicated by an additional component associated with recirculating flow. With more theoretical studies, new experiments can be performed to test theoretical predictions. Such theoretical and experimental studies would be useful for improving the chemistrode and for understanding other phenomena that involve diffusional transfer in multiphase or recirculating flows near surfaces.

Acknowledgments

This research was supported by the NIH Director's Pioneer Award 1DP1OD003584 and the NSF CRC CHE-0526693. RFI is a Cottrell Scholar of Research Corporation and a Camille Dreyfus Teacher-Scholar. A part of this work was performed at the MRSEC microfluidic facility funded by the NSF. We thank Elizabeth B Haney for contributions in English corrections and editing this manuscript.

References

[1] Chen D, Du W B, Liu Y, Liu W S, Kuznetsov A, Mendez F E, Philipson L H and Ismagilov R F 2008 The chemistrode: a droplet-based microfluidic device for stimulation and recording with high temporal, spatial, and chemical resolution *Proc. Natl Acad. Sci. USA* **105** 16843–8

[2] Wang M, Roman G T, Schultz K, Jennings C and Kennedy R T 2008 Improved temporal resolution for *in vivo* microdialysis by using segmented flow *Anal. Chem.* **80** 5607–15

[3] Sahoo H R, Kralj J G and Jensen K F 2007 Multistep continuous-flow microchemical synthesis involving multiple reactions and separations *Angew. Chem. Int. Ed. Engl.* **46** 5704–8

[4] Garstecki P, Fuerstman M J, Stone H A and Whitesides G M 2006 Formation of droplets and bubbles in a microfluidic T-junction—scaling and mechanism of break-up *Lab Chip* **6** 437–46

[5] Link D R, Grasland-Mongrain E, Duri A, Sarrazin F, Cheng Z D, Cristobal G, Marquez M and Weitz D A 2006 Electric control of droplets in microfluidic devices *Angew. Chem. Int. Ed. Engl.* **45** 2556–60

[6] Lorenz R M, Edgar J S, Jeffries G D M and Chiu D T 2006 Microfluidic and optical systems for the on-demand generation and manipulation of single femtoliter-volume aqueous droplets *Anal. Chem.* **78** 6433–9

[7] Fidalgo L M, Abell C and Huck W T S 2007 Surface-induced droplet fusion in microfluidic devices *Lab Chip* **7** 984–6

[8] Anna S L, Bontoux N and Stone H A 2003 Formation of dispersions using 'flow focusing' in microchannels *Appl. Phys. Lett.* **82** 364–6
[9] Fidalgo L M, Whyte G, Bratton D, Kaminski C F, Abell C and Huck W T S 2008 From microdroplets to microfluidics: selective emulsion separation in microfluidic devices *Angew. Chem. Int. Ed. Engl.* **47** 2042–5
[10] Liu Y and Ismagilov R F 2009 Dynamics of coalescence of plugs with a hydrophilic wetting layer induced by flow in a microfluidic chemistrode *Langmuir* **25** 2854–9
[11] Yoon Y, Borrell M, Park C C and Leal L G 2005 Viscosity ratio effects on the coalescence of two equal-sized drops in a two-dimensional linear flow *J. Fluid Mech.* **525** 355–79
[12] Shestopalov I, Tice J D and Ismagilov R F 2004 Multi-step synthesis of nanoparticles performed on millisecond time scale in a microfluidic droplet-based system *Lab Chip* **4** 316–21
[13] Axelrod D 2001 Total internal reflection fluorescence microscopy in cell biology *Traffic* **2** 764–74
[14] Duffy D C, McDonald J C, Schueller O J A and Whitesides G M 1998 Rapid prototyping of microfluidic systems in poly(dimethylsiloxane) *Anal. Chem.* **70** 4974–84
[15] Lide D R (ed) 2003 *CRC Handbook of Chemistry and Physics* 84th edn (Boca Raton, FL: CRC Press)
[16] Roach L S, Song H and Ismagilov R F 2005 Controlling nonspecific protein adsorption in a plug-based microfluidic system by controlling interfacial chemistry using fluorous-phase surfactants *Anal. Chem.* **77** 785–96
[17] Pristinski D, Kozlovskaya V and Sukhishvili S A 2005 Fluorescence correlation spectroscopy studies of diffusion of a weak polyelectrolyte in aqueous solutions *J. Chem. Phys.* **122**
[18] Dean R B and Loring H S 1945 The diffusion of organic ions and the Einstein–Sutherland relationship *J. Biol. Chem.* **157** 717–21
[19] Bringer M R, Gerdts C J, Song H, Tice J D and Ismagilov R F 2004 Microfluidic systems for chemical kinetics that rely on chaotic mixing in droplets *Phil. Trans. R. Soc.* A **362** 1087–104
[20] Ottino J M and Wiggins S 2004 Applied physics—designing optimal micromixers *Science* **305** 485–6
[21] Song H, Bringer M R, Tice J D, Gerdts C J and Ismagilov R F 2003 Experimental test of scaling of mixing by chaotic advection in droplets moving through microfluidic channels *Appl. Phys. Lett.* **83** 4664–6
[22] Stroock A D, Dertinger S K W, Ajdari A, Mezic I, Stone H A and Whitesides G M 2002 Chaotic mixer for microchannels *Science* **295** 647–51
[23] Ottino J M and Wiggins S 2004 Introduction: mixing in microfluidics *Phil. Trans. R. Soc.* A **362** 923–35
[24] Wiggins S and Ottino J M 2004 Foundations of chaotic mixing *Phil. Trans. R. Soc.* A **362** 937–70
[25] Leveque M A 1928 Les lois de la transmission de chaleur par convection *Ann. Mines* **13** 201
[26] Ismagilov R F, Stroock A D, Kenis P J A, Whitesides G and Stone H A 2000 Experimental and theoretical scaling laws for transverse diffusive broadening in two-phase laminar flows in microchannels *Appl. Phys. Lett.* **76** 2376–8
[27] Ghosh S, Leonard A and Wiggins S 1998 Diffusion of a passive scalar from a no-slip boundary into a two-dimensional chaotic advection field *J. Fluid Mech.* **372** 119–63
[28] Kirtland J D, McGraw G J and Stroock A D 2006 Mass transfer to reactive boundaries from steady three-dimensional flows in microchannels *Phys. Fluids* **18** 073602